

LETHE: Adapter-Augmented Dual-Stream Update for Persistent Knowledge Erasure in Federated Unlearning

Hanwei Tan¹, Wentai Wu¹, Ligang He², and Yijun Quan²

¹Jinan University

²University of Warwick

^{*}tanhanyiwei@jnu.edu.cn, wentaiwu@jnu.edu.cn, ligang.he@warwick.ac.uk,
yijun.quan@warwick.ac.uk

February 2, 2026

Abstract

Federated unlearning (FU) aims to erase designated client-level, class-level, or sample-level knowledge from a global model. Existing studies commonly assume that the collaboration ends up with the unlearning operation, overlooking the follow-up situation where the federated training continues over the remaining data. We identify a critical failure mode, termed *Knowledge resurfacing*, by revealing that continued training can re-activate unlearned knowledge and cause the removed influence to resurface in the global model. To address this, we propose LETHE, a novel federated unlearning method that de-correlates knowledge to be unlearned from knowledge to be retained, ensuring persistent erasure during continued training. LETHE follows a Reshape–Rectify–Restore pipeline: a temporary adapter is first trained with gradient ascent on the unlearning data to obtain magnified updates, which is then used as corrective signals to diverge layer-wise rectification on the remaining updates in two streams. Finally, the adapter is removed and a short recovery stage is performed on the retained data. Our experiments show that LETHE supports unlearning in the federated system at all levels in a unified manner and maintains superior persistence (Resurfacing Rate <1% in most cases) even after numerous rounds of follow-up training.

1 Introduction

Federated learning (FL) enables distributed clients to collaboratively train models without sharing raw data [20]. In practical deployments, however, a trained global model may still retain undesired influence from specific clients or data samples [12, 4]. Motivated by the strict compliance with privacy regulations (e.g., the “Right to be Forgotten”) and the obligation to adhere to user-initiated unlearning protocols, Federated Unlearning (FU) aims to remove the influence of designated clients, classes, or samples from a trained model [12]. While retraining from scratch on the remaining data is a straightforward option, it is often prohibitive in computation/communication cost and latency at scale. As a result, most FU methods pursue *approximate unlearning*, aiming to efficiently update the model so that its behavior closely matches a reference model retrained on the remaining dataset with the target data removed [15].

In practice, unlearning is rarely the terminal operation: once an unlearning request is served, federated training typically resumes on the remaining clients to complete or further improve the model. However, as soon as training continues on the remaining data \mathcal{D}_r , the model may relearn the removed influence within only a few additional communication rounds, causing unlearned patterns to re-surface. Figure 1 highlights this post-unlearning failure mode that we term *knowledge resurfacing*. Related evidence from large-model

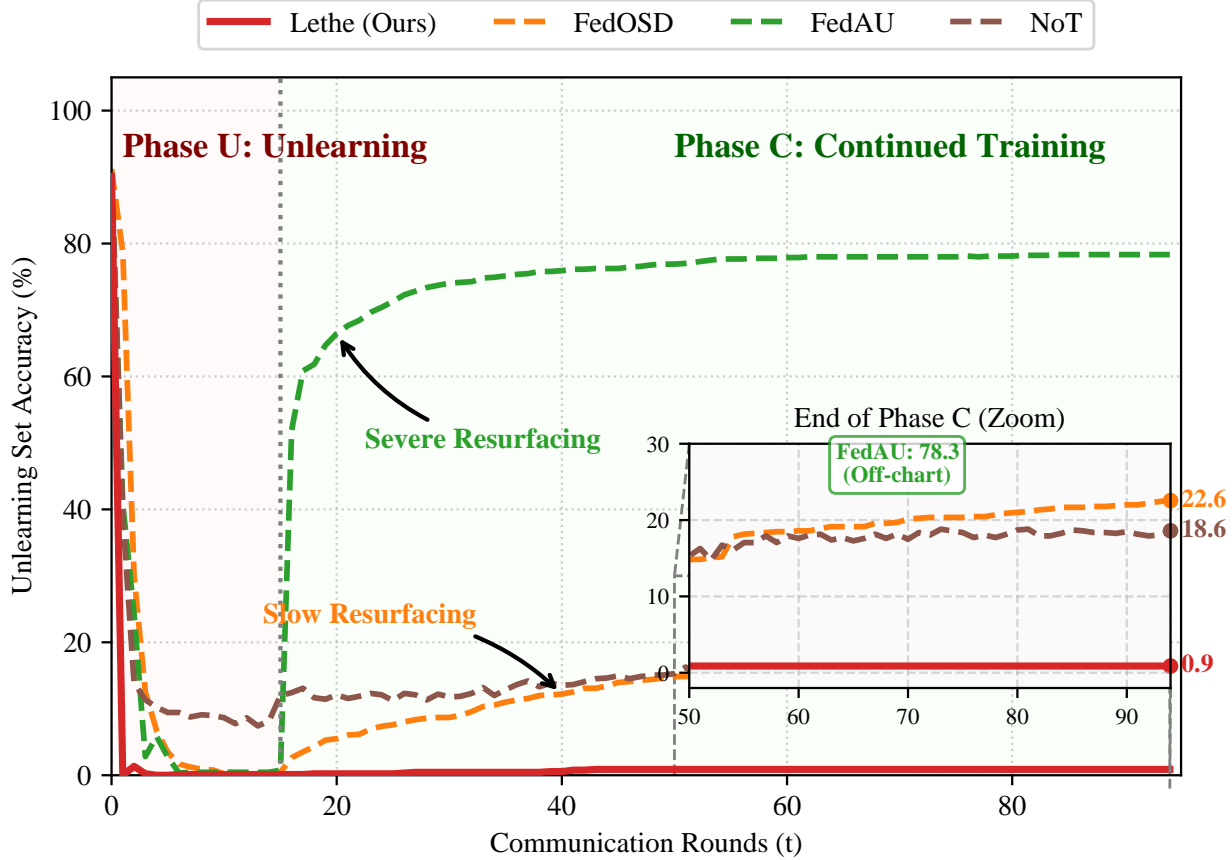


Figure 1: The effect of unlearning, characterized by unlearning set accuracy (lower is better), may not persist. SOTA methods proved effective in unlearning (Phase U) are susceptible to knowledge resurfacing during continued training (Phase C). The proposed LETHE (red) unlearns efficiently and stays that way (inset).

unlearning also shows that even benign post-unlearning fine-tuning can trigger the reappearance of removed influence [7], suggesting that this phenomenon is not a federated-specific edge case but a broader challenge for unlearning methods.

To address this, We propose LETHE, a federated unlearning method for *persistent* forgetting that stays uncompromised during continued training. To quantitatively measure this persistence, we introduce the *Resurfacing Rate (RR)*, which measures how much of the forgotten influence re-emerges during continued training. Our key contributions are as follows:

- **Metric and analysis:** We trace inference accuracy on the unlearning set and introduce the *Resurfacing Rate (RR)* as a quantitative measure of knowledge resurfacing during continued training. We also provide theoretical analysis to reveal why unlearned knowledge resurfaces under certain assumptions.
- **Methodology:** We propose LETHE, a federated unlearning method based on adapter-augmented knowledge de-correlation, which effectively suppresses knowledge resurfacing at all levels even after numerous rounds of follow-up training.
- **Evaluation:** LETHE consistently achieves near-zero resurfacing ($RR < 1\%$ in most cases) across diverse settings, outperforming existing baselines while maintaining competitive utility.

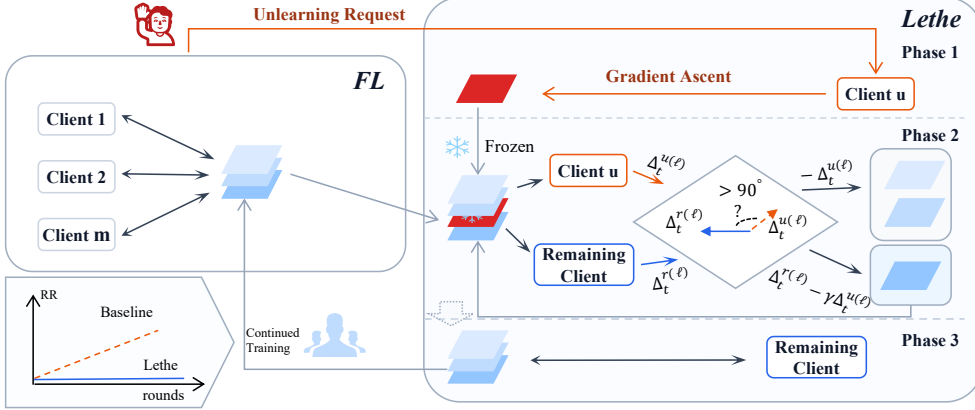


Figure 2: **LETHE for persistent federated unlearning.** LETHE takes action in the unlearning phase and follows a Reshape–Rectify–Restore pipeline: an adapter-based probe extracts Δ^u on \mathcal{D}_u , followed by dual-stream update rectification and adapter removal. In our scenario, federated training will subsequently resume on remaining clients, during which knowledge resurfacing is undesirable.

2 Related Work

We review existing FU methods in three categories.

Historical trajectory-based FU. This category seeks to approximate the retraining-from-scratch baseline by “rewinding” the optimization trajectory. FedEraser [13] reconstructs historical updates via iterative unrolling on retained data, while FedRecovery [22] utilizes stored gradient residuals for post-hoc correction. However, these methods suffer from prohibitive storage complexity and computational overhead, especially in long-horizon training where replaying/correcting extensive trajectories becomes a bottleneck for real-time deployment.

FU based on modular update. Modular FU avoids full retraining by isolating updates to specialized parameters. FedAU [3] employs linear neutralization, and FUSED [23] leverages LoRA-based overwriting. Despite their efficiency, these methods typically leave the pre-trained backbone untouched. Consequently, unlearned representations are often masked rather than erased, allowing latent knowledge to persist in the backbone and potentially trigger knowledge resurfacing during subsequent model updates or module removals.

FU based on update correction. These approaches directly modify model weights to satisfy unlearning objectives. NoT [8] employs weight-negation and fine-tuning; while efficient, it often yields incomplete forgetting. FedOSD [16] introduces orthogonal steepest descent to mitigate unwanted relearning by projecting updates onto a space orthogonal to the unlearning client’s gradients. Nevertheless, these ad hoc optimization constraints often fail to provide long-term stability; as standard federated training resumes, the global model tends to re-accumulate forgotten components, leading to a degradation of the unlearning effect over time.

In summary, current FU methods face a critical dilemma between efficiency and persistence. Historical trajectory-based methods offer high fidelity but are hindered by impractical overhead, while optimization-based approximations achieve efficiency at the cost of unlearning persistence. Most lightweight methods rely on transient masks or local constraints that are easily overridden by subsequent training on remaining clients,

leading to the knowledge resurfacing phenomenon. LETHE seeks to bridge this gap by enabling efficient unlearning while maintaining persistent forgetting under continued training.

3 Preliminaries and Problem Formulation

In this section, we revisit the basics of FL and connect it to the most fundamental FU approach based on retraining. Then, we formulate the problem of FU considering both the unlearning phase and the continued training phase. Finally, we define the measure of Resurfacing Rate.

3.1 Federated Learning and Clean Retraining

We consider an FU scenario involving two back-to-back phases: unlearning phase (Phase U) and continued training phase (Phase C). Federated learning is presumably run in the first place before unlearning as well as in the Phase C. In addition, we also take FL as a retraining baseline in which the unlearning set \mathcal{D}_u is never used when the clients collaboratively retrain towards a “clean” global model. For client-level unlearning, this reduces to retraining on the remaining clients. Concretely, given an unlearning request specifying the unlearning client set $\mathcal{K}_f \subseteq \mathcal{K}$, we define the remaining client set $\mathcal{K}_r \triangleq \mathcal{K} \setminus \mathcal{K}_f$. Thus the most straightforward FU is to retrain a global model over $\{\mathcal{D}_k\}_{k \in \mathcal{K}_r}$ using the vanilla FedAvg protocol [14]. For sample-level and class-level unlearning, retraining follows the same protocol while keeping the same client set, but filters each participating client’s local dataset to exclude the target samples/classes.

Let $n_k = |\mathcal{D}_k|$ and $N_r = \sum_{k \in \mathcal{K}_r} n_k$ be the total number of samples on remaining clients. Let $\mathbf{w}^{(\ell)} \in \mathbb{R}^d$ denote the parameter vector of layer ℓ . At round t , the retraining server update is

$$\mathbf{w}_{t+1}^{(\ell)} = \mathbf{w}_t^{(\ell)} + \sum_{k \in \mathcal{K}_r} q_k \Delta \mathbf{w}_{t,k}^{(\ell)}, \quad (1)$$

where $\Delta \mathbf{w}_{t,k}^{(\ell)} \triangleq \mathbf{w}_{t,k}^{(\ell)} - \mathbf{w}_t^{(\ell)}$ is the local update from remaining client k , and $q_k = \frac{n_k}{N_r}$ is the normalized aggregation weight over remaining clients. We treat the resulting re-trained model as the gold-standard reference for optimal forgetting, and evaluate unlearning methods by how closely they match this outcome while maintaining utility and efficiency.

Granularity of FU Federated unlearning can be categorized by the granularity of knowledge to be forgotten: (1) *Sample unlearning*: remove the influence of specified samples from a client. (2) *Client unlearning*: erase the contribution of all local data from a designated client. (3) *Class unlearning*: remove knowledge associated with a target class, where the target data are typically distributed across many or all clients.

3.2 Problem Formulation

Let $\mathcal{D} = \mathcal{D}_r \cup \mathcal{D}_u$ denote the global dataset, where \mathcal{D}_u is the designated unlearning set and \mathcal{D}_r is the remaining set. We first train a global model on \mathcal{D} , yielding \mathbf{w}_{pre} .

$$\mathbf{w}_{\text{pre}} = \arg \min_{\mathbf{w}} \mathcal{L}(\mathbf{w}; \mathcal{D}). \quad (2)$$

Clean retraining (reference). The desired reference after removing \mathcal{D}_u is the model obtained by retraining on the remaining set only:

$$\mathbf{w}_{\text{re}} = \arg \max_{\mathbf{w}} \mathcal{L}(\mathbf{w}; \mathcal{D}_r). \quad (3)$$

Phase U objective. Given a global model \mathbf{w}_{pre} and an unlearning set \mathcal{D}_u specified by an unlearning request, a federated unlearning algorithm \mathcal{A} outputs an unlearned model:

$$\mathbf{w}_{\text{un}} \triangleq \mathcal{A}(\mathbf{w}_{\text{pre}}; \mathcal{D}_u, \mathcal{D}_r). \quad (4)$$

which should both preserve utility on the remaining set and forget \mathcal{D}_u , matching the retraining reference \mathbf{w}_{re} in behavior. Concretely, we require (i) *utility preservation*: high test accuracy on a held-out test set (close to \mathbf{w}_{re}), and (ii) *forgetting*: minimum performance on \mathcal{D}_u comparable to clean retraining. Equivalently, Phase U seeks a model that minimizes remaining-data loss while meeting a forgetting threshold:

$$\mathbf{w}_{\text{un}} \approx \arg \min_{\mathbf{w}} \mathcal{L}_r(\mathbf{w}; \mathcal{D}_r) \quad \text{s.t.} \quad \mathcal{L}_u(\mathbf{w}) \geq \tau_f, \quad (5)$$

where τ_f specifies the desired level of forgetting.

Phase C requirement (persistence). Let \mathbf{w}_{cont} be the model after T_{cont} rounds of continued training on the remaining set. We require forgetting to persist while the model does not deteriorate:

$$\mathcal{L}_u(\mathbf{w}_{\text{cont}}) \geq \tau_f, \text{ and } \mathcal{L}_r(\mathbf{w}_{\text{cont}}; \mathcal{D}_r) \leq \mathcal{L}_r(\mathbf{w}_{\text{un}}; \mathcal{D}_r). \quad (6)$$

3.3 Measure of Knowledge Resurfacing

Inference accuracy on the unlearning set is a basic indicator of FU’s effectiveness:

$$A_f \triangleq \mathbb{E}_{(x,y) \sim \mathcal{D}_u} [\mathbf{1}\{f(x) = y\}]. \quad (7)$$

In our scenario, we pay attention to A_f before, during and after the Phase C to characterize the effect of knowledge resurfacing. Let A_f^{pre} , A_f^U , and A_f^C denote the A_f measured before unlearning, right after Phase U, and during continued training in Phase C, respectively. We define RR :

$$\text{RR} \triangleq \frac{\max(0, A_f^C - A_f^U)}{A_f^{\text{pre}} - A_f^U} \times 100\%, \quad (8)$$

Note that RR is reported only when A_f^U is relatively close to the retraining baseline, otherwise it is marked as **unsuccessful forgetting (UF)**.

4 Methodology

Why knowledge resurfacing happens. After unlearning, federated training typically continues on the remaining data \mathcal{D}_r . Geometrically, knowledge resurfacing arises when remaining clients’ updates have a non-trivial projection onto the unlearning direction, so the aligned components accumulate through continued training on \mathcal{D}_r and gradually reconstruct the forgotten patterns. This matches recent observations that post-unlearning continued training can trigger resurfacing without explicit de-correlation of the erased influence [7]. In fig. 3 we visualize the correlation of updates on the unlearning set and the remaining set, which helps understand how knowledge resurfacing happens. Starting from the unlearning model \mathbf{w}_{un} , we run FL on the remaining clients and obtain the aggregated update $\Delta_r^{(t,\ell)}$ at each round t for layer ℓ . As a diagnostic reference, we compute a fixed unlearning update $\Delta_u^{(\ell)}$ once at \mathbf{w}_{pre} on \mathcal{D}_u . Each cell reports the time-averaged correlation score $c^{(\ell)} = \frac{1}{T} \sum_{t=0}^{T-1} \cos(\Delta_r^{(t,\ell)}, \Delta_u^{(\ell)})$. Consistently positive correlation in deep layers indicates a non-trivial component shared by the two types of updates, which gradually reconstructs unlearned patterns.

Algorithm 1 LETHE

- 1: **Input:** Initial global model \mathbf{w}_{pre} ; unlearning clients \mathcal{C}_u ; remaining clients \mathcal{C}_r ; correlation penalty γ ; unlearning set \mathcal{D}_u ; remaining set \mathcal{D}_r .
- 2: **Output:** Unlearned model \mathbf{w}^* .
- 3: $\mathbf{w}_0 \leftarrow \mathbf{w}_{\text{pre}}$.
- 4: // Phase 1: Reshape (Probe Adapter Training)
- 5: Server freezes backbone \mathbf{w}_0 , initializes adapter ϕ .
- 6: Unlearning clients \mathcal{C}_u perform gradient ascent on ϕ :
- 7: $\phi^* \leftarrow \phi + \nabla_\phi \mathcal{L}(\mathbf{w}_0, \phi; \mathcal{D}_u)$
- 8: Server freezes ϕ^* .
- 9: // Phase 2: Rectify (Dual-Stream Rectification)
- 10: **for** $t = 0$ to $T_{\text{unlearn}} - 1$ **do**
- 11: Server broadcasts \mathbf{w}_t and frozen ϕ^* .
- 12: // Forget stream (corrective signal):
- 13: $\Delta_t^u \leftarrow \text{LocalTrain}(\mathbf{w}_t, \text{frozen } \phi^*; \mathcal{D}_u) - \mathbf{w}_t$
- 14: // Retained stream (utility):
- 15: Sample $\mathcal{B}_t \subset \mathcal{C}_r$,
- 16: $\Delta_t^r \leftarrow \sum_{k \in \mathcal{B}_t} p_k(\text{LocalTrain}(\mathbf{w}_t; \mathcal{D}_k) - \mathbf{w}_t)$
- 17: **for** each layer ℓ **do**
- 18: $\text{sim}_t^{(\ell)} \leftarrow \langle \Delta_t^{r,(\ell)}, \Delta_t^{u,(\ell)} \rangle$
- 19: **if** $\text{sim}_t^{(\ell)} > 0$ **then**
- 20: $\tilde{\Delta}_t^{(\ell)} \leftarrow \Delta_t^{r,(\ell)} - \gamma \Delta_t^{u,(\ell)}$
- 21: **else**
- 22: $\tilde{\Delta}_t^{(\ell)} \leftarrow -\Delta_t^{u,(\ell)}$
- 23: **end if**
- 24: **end for**
- 25: $\mathbf{w}_{t+1} \leftarrow \mathbf{w}_t + \tilde{\Delta}_t$
- 26: **end for**
- 27: // Phase 3: Restore (Utility Recovery)
- 28: Remove adapter ϕ^* . Run R rounds of FedAvg on \mathcal{C}_r .
- 29: **return** \mathbf{w}^* .

Theoretical analysis. In Proposition 4.1 we prove that the unlearning-set loss upper bound decreases in continued training under certain assumptions, which implies that knowledge resurfacing occurs. The key condition here is that the unlearning-set gradient $g_u = \nabla \mathcal{L}_u(\mathbf{w}_{\text{pre}})$ has a persistently positive average inner product with the Phase-C gradients $\{g_r^{(t)} = \nabla \mathcal{L}_r(\mathbf{w}_t)\}_{t=1}^T$ on remaining data. We estimate this condition via update correlation: let $\Delta_r^{(t,\ell)}$ be the aggregated update at continued-training round t in layer ℓ , and let $\Delta_u^{(\ell)}$ be a fixed reference unlearning update computed once at \mathbf{w}_{pre} on \mathcal{D}_u . We define $c^{(t,\ell)} \triangleq \cos(\Delta_r^{(t,\ell)}, \Delta_u^{(\ell)})$, whose time average proxies $\frac{1}{T} \sum_t \mathbb{E} \langle g_u, g_r^{(t)} \rangle$.

Proposition 4.1 (Knowledge Resurfacing with Smoothness-Controlled Drift). *Let $\mathcal{L}_u(w)$ and $\mathcal{L}_r(w)$ be the losses on the unlearning set \mathcal{D}_u and the remaining set \mathcal{D}_r . After unlearning, consider continued training on \mathcal{D}_r :*

$$w_{t+1} = w_t - \eta g_r^{(t)}, \quad g_r^{(t)} := \nabla \mathcal{L}_r(w_t).$$

Fix \mathbf{w}_{pre} and denote $g_u := \nabla \mathcal{L}_u(\mathbf{w}_{\text{pre}})$. Assume: (i) \mathcal{L}_u is β -smooth; (ii) $\|g_r^{(t)}\| \leq G$; and (iii) there exists

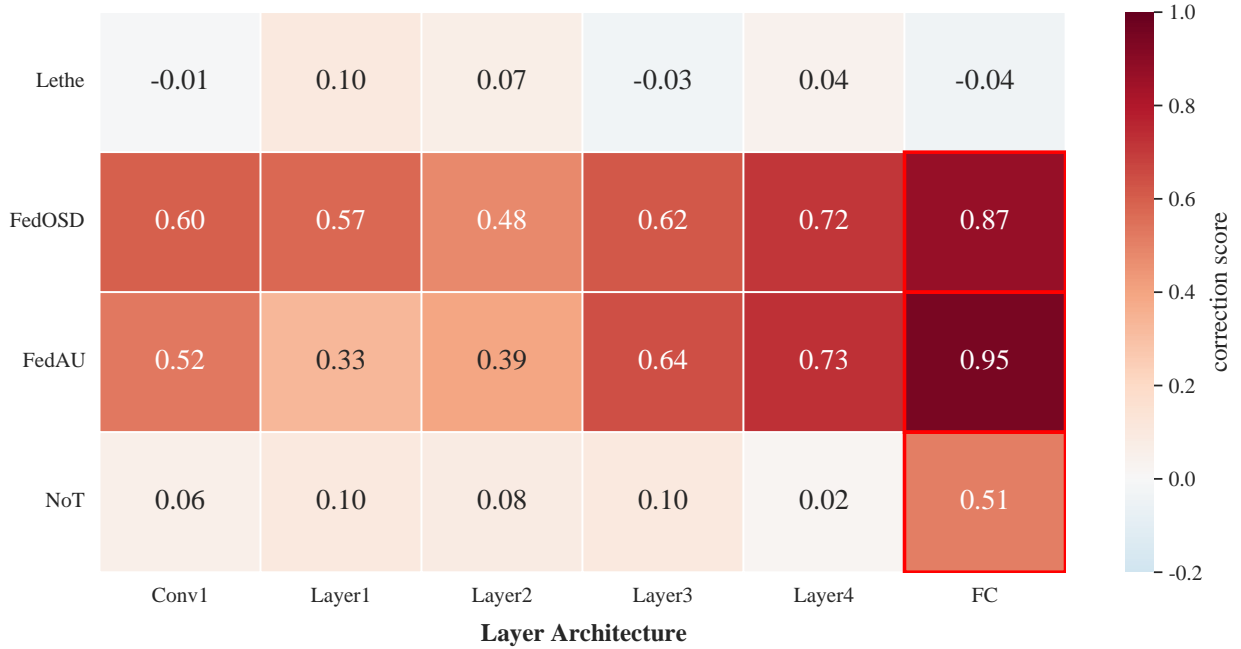


Figure 3: Visualization of the layer-wise correlation score $c^{(\ell)} = \frac{1}{T} \sum_{t=0}^{T-1} \cos(\Delta_r^{(t,\ell)}, \Delta_u^{(\ell)})$ during continued federated training. Darker color indicates higher alignment of updates in the vector space. Existing algorithms fail to de-correlate the updates on the unlearning set and remaining set especially in the deep layers.

$\rho > 0$ such that the average alignment satisfies

$$\frac{1}{T} \sum_{t=0}^{T-1} \mathbb{E}[\langle g_u, g_r^{(t)} \rangle] \geq \rho.$$

Then for any $T \geq 1$,

$$\mathbb{E}[\mathcal{L}_u(w_T)] \leq \mathcal{L}_u(w_{pre}) - \eta \rho T + \frac{\beta \eta^2 G^2}{2} T^2.$$

In particular, \mathcal{L}_u decreases (i.e., erased influence resurfaces) whenever $T < \frac{2\rho}{\beta \eta G^2}$.

Proof. See Appendix A.

Figure 3 shows consistently positive correlation in deep layers for standard baselines, supporting $\rho > 0$ and the resurfacing condition in the Proposition.

4.1 The LETHE Method

LETHE enforces the de-correlating manipulation in the update space by using the model update on the unlearning set as a reference signal to rectify the server-aggregated update, which makes the model learn to decouple the unlearning set knowledge from the remaining set knowledge.

Phase 1: Reshape (Probe Adapter Training on the unlearning Client). We attach a lightweight adapter ϕ to the global backbone \mathbf{w} and freeze the backbone. On the unlearning client, we train the adapter via gradient ascent on the unlearning data \mathcal{D}_u to obtain a stable probe ϕ^* :

$$\phi^* \leftarrow \phi + \nabla_{\phi} \mathcal{L}(\mathbf{w}, \phi; \mathcal{D}_u), \quad (9)$$

where \mathbf{w} remains frozen during this phase. We then freeze ϕ^* for subsequent rounds.

Phase 2: Rectify (Dual-Stream Updates and Layer-wise Rectification). At each round t , we temporarily plug the frozen probe adapter ϕ^* into the global model, followed by two streams of local update:

(1) *Forget stream (corrective signal)*. The unlearning client computes a local backbone update on \mathcal{D}_u using the composite model (with ϕ^* frozen):

$$\Delta_t^u \triangleq \text{LocalTrain}(\mathbf{w}_t, \text{frozen } \phi^*; \mathcal{D}_u) - \mathbf{w}_t. \quad (10)$$

(2) *Retain stream (utility direction)*. Simultaneously, remaining clients perform local training on their private data \mathcal{D}_r (with ϕ^* frozen). The server aggregates their backbone updates to form the retained direction Δ_t^r .

(3) *Layer-wise rectification*. For each layer ℓ , we at the server compute a layer-wise similarity score

$$\text{sim}_t^{(\ell)} \triangleq \left\langle \Delta_t^{r,(\ell)}, \Delta_t^{u,(\ell)} \right\rangle, \quad (11)$$

and apply the following conditional rectification rule:

$$\tilde{\Delta}_t^{(\ell)} = \begin{cases} \Delta_t^{r,(\ell)} - \gamma \Delta_t^{u,(\ell)} & \text{if } \text{sim}_t^{(\ell)} > 0, \\ -\Delta_t^{u,(\ell)} & \text{if } \text{sim}_t^{(\ell)} \leq 0, \end{cases} \quad (12)$$

where γ is the correlation penalty (see Appendix D for details). The backbone is updated by $\mathbf{w}_{t+1}^{(\ell)} = \mathbf{w}_t^{(\ell)} + \tilde{\Delta}_t^{(\ell)}$.

Phase 3: Restore (Adapter Removal and Retained Recovery). After T rectification rounds, we discard the probe adapter ϕ^* and run R rounds of standard FedAvg on remaining clients to restore utility:

$$\mathbf{w}_{t+1} \leftarrow \mathbf{w}_t + \Delta_t^r, \quad t = T, \dots, T + R - 1. \quad (13)$$

4.2 Theoretical analysis

First-order justification and connection to resurfacing. Proposition 4.1 shows that *knowledge resurfacing* is caused by persistent positive alignment between the updates during continued training and the unlearning direction, i.e., $\frac{1}{T} \sum_t \mathbb{E} \langle g_u, g_r^{(t)} \rangle \geq \rho > 0$. LETHE therefore treats the unlearning client's local update as an unlearning-direction signal and explicitly alleviates correlation by rectifying the aggregated r-set update via subtraction and negation. Inspired by existing studies [4, 16, 21], Proposition 4.2 provides a first-order justification: the rule either (i) removes the positive projection of the retained update onto the unlearning direction when such correction exists (subtraction), or (ii) takes a negation step that increases the unlearning loss while remaining non-adversarial to utility when the two updates are not positively correlated

Proposition 4.2 (Client-update subtraction/negation suppresses correction to first order). *In round t for any layer ℓ , without loss of generality, we assume linearized approximation of local updates $\Delta_t^{u,(\ell)} \approx -\eta_u \nabla_{\mathbf{w}^{(\ell)}} \mathcal{L}_u(\mathbf{w}_t)$ and $\Delta_t^{r,(\ell)} \approx -\eta_r \nabla_{\mathbf{w}^{(\ell)}} \mathcal{L}_r(\mathbf{w}_t)$, and apply the rectified rule by Eq (12), then it holds that*

(i) (Effectiveness of forgetting) $\mathcal{L}_u(\mathbf{w}_{t+1}) - \mathcal{L}_u(\mathbf{w}_t)$ increases to first order whenever $\langle \Delta_t^{u,(\ell)}, \tilde{\Delta}_t^{(\ell)} \rangle \leq 0$ for all ℓ ;

(ii) (Preservation of utility) $\langle \Delta_t^{r,(\ell)}, \tilde{\Delta}_t^{(\ell)} \rangle \geq 0$ if $\langle \Delta_t^{r,(\ell)}, \Delta_t^{u,(\ell)} \rangle \leq 0$.

The full proof is deferred to Appendix B.1.

Table 1: Results of client-level unlearning. w_{pre} denotes the model before unlearning; superscripts U and C report results measured after Phase U and after Phase C, respectively. For HSViT (Pat-50), communication rounds for the two phases are reported by T_U/T_P . The best results are marked in **bold**.

Algorithm	LeNet5				ResNet18				HSViT		
	Pat-10		Pat-50		Pat-10		Pat-50		Pat-50		
	u-Acc ↓	t-Acc	T_U/T_P	u-Acc ↓	t-Acc						
w_{pre}	96.06±3.05	98.18	98.99±0.36	97.86	95.40±1.25	66.37	90.77±7.16	59.97	-	91.65±0.57	48.73
Retraining	0.12±0.05	97.44	0.31±0.17	97.59	2.48±0.94	65.33	3.04±1.03	58.72	1000	0.47±0.02	49.85
FedEraser	0.10±0.01	98.45	0.25±0.04	97.93	1.52±0.43	70.01	3.44±0.96	64.45	-	-	-
FedAU ^U	0.46±0.09	94.87	0.62±0.04	96.32	0.21±0.04	60.63	0.00±0.00	58.26	40/0	0.35±0.22	48.68
FedOSD ^U	0.89±0.00	97.44	0.65±0.00	97.73	0.78±0.00	67.18	0.56±0.00	65.93	23/32	0.36±0.31	10.66
NoT ^U	1.02±0.00	95.12	1.02±0.00	94.02	21.89±0.00	65.96	35.78±0.00	57.73	0/40	0.55±0.25	46.97
ours ^U	0.27±0.19	95.79	0.22±0.04	95.35	0.10±0.04	64.68	0.11±0.00	57.84	20/10	0.10±0.07	47.41
After continued training (Phase C)											
FedAU ^C	34.90±24.37	98.59	49.37±1.62	98.34	89.85±1.25	69.67	90.63±0.58	65.90	-	21.73±6.98	49.67
FedOSD ^C	10.86±2.77	98.65	4.18±0.13	98.45	60.04±6.02	70.35	67.48±3.09	67.87	-	63.62±4.80	45.89
NoT ^C	0.48±0.06	98.31	0.37±0.00	97.73	29.11±3.77	68.10	20.78±1.10	63.45	-	0.60±0.31	48.46
ours ^C	0.15±0.08	98.52	0.34±0.22	98.03	0.24±0.20	69.32	1.15±0.52	65.05	-	0.45±0.37	49.29

5 Experiments

5.1 Experimental Setting

Models and datasets. We performed evaluation on MNIST [11] with LeNet-5 [11], CIFAR-10 [9] with ResNet-18 [5], and Tiny-ImageNet [1, 10] with HSViT [19].

Evaluation protocol. We evaluate whether an unlearning method (i) effectively removes the influence of the target client data and (ii) remains robust to *knowledge resurfacing* under continued training. Following prior federated unlearning (FU) evaluations [4, 3, 16], we consider both IID and Non-IID client data partitions. For the Non-IID setting, we partition the data to generate heterogeneous client label proportions by employing a Dirichlet distribution $\text{Dir}(\alpha)$ with a concentration parameter $\alpha = 0.1$ [6]. We further vary the federation scale with $K \in \{10, 50\}$ clients, denoted as Pat-10 and Pat-50. We also conduct experiments under IID settings; full experimental details are deferred to the Appendix C.

Unlearning targets. We instantiate the unlearning set \mathcal{D}_u using a backdoor injection protocol [2]. For *sample unlearning*, we set the forget ratio as $|\mathcal{D}_u|/|\mathcal{D}| \in \{1\%, 5\%, 10\%, 20\%\}$. For *client unlearning*, \mathcal{D}_u consists of all local data of the designated client. For *class unlearning*, we do not use backdoor triggers and instead forget the samples from class 0 by default.

Baselines and hyperparameters. We compare against both retraining-based baselines and state-of-the-art FU approaches. Clean retraining is implemented using FedAvg and we also include FedEraser, a retraining-based acceleration method that reuses statistics of historical local updates recorded during the original FL run. For representative FU baselines, we include FedAU, FedOSD, and NoT. Note that FedOSD is designed only for client-level unlearning and thus is only evaluated on client unlearning settings. FedEraser

Table 2: Results of sample-level and class-level unlearning. The w_{pre} denotes the model before unlearning; superscripts U and C report results measured after Phase U and Phase C, respectively. The best results are marked in **bold**.

Algorithm	Sample Unlearning								Class Unlearning			
	1% Sample		5% Sample		10% Sample		20% Sample		Client-10		Client-50	
	u-Acc ↓	t-Acc	u-Acc ↓	t-Acc	u-Acc ↓	t-Acc	u-Acc ↓	t-Acc	u-Acc ↓	t-Acc	u-Acc ↓	t-Acc
w_{pre}	100.00±0.00	82.51	99.71±0.41	82.15	99.85±0.21	82.38	99.71±0.34	82.16	100.00±0.00	77.88	100.00±0.00	71.61
Retraining	0.66±0.93	77.63	1.73±0.58	77.36	2.02±0.17	77.26	1.90±0.09	77.12	0.00±0.00	76.77	0.00±0.00	71.13
FedAU ^U	0.00±0.00	69.04	0.03±0.04	60.58	0.00±0.00	63.17	0.00±0.00	70.70	0.00±0.00	78.44	0.00±0.00	63.53
NoT ^U	21.98±10.69	78.64	30.27±14.09	78.69	15.31±3.09	78.29	23.42±10.22	77.80	0.00±0.00	78.86	0.00±0.00	70.37
ours ^U	0.32±0.45	82.20	0.96±0.51	81.66	0.91±0.35	82.04	0.99±0.39	81.93	0.00±0.00	79.01	0.00±0.00	72.00
After continued training (Phase C)												
FedAU ^C	64.44±29.37	82.80	87.13±8.05	82.50	90.15±2.93	82.49	91.99±1.72	82.15	0.00±0.00	78.51	0.00±0.00	72.46
NoT ^C	30.80±9.62	79.65	43.19±7.97	79.62	38.73±3.50	79.60	50.69±15.67	79.23	10.19±1.86	81.05	3.11±0.71	75.21
ours ^C	0.51±0.72	82.46	1.29±0.67	82.01	1.73±0.12	82.33	1.34±0.41	81.95	0.00±0.00	78.71	0.00±0.00	72.17

accelerates retraining by caching historical client updates, but these update tensors are too large for HSViT on Tiny-ImageNet to store across rounds under our hardware budget, so we omit FedEraser for this setting.

Metrics and efficiency. All metrics are evaluated on held-out **test** splits. We report **t-Acc** as the clean test accuracy on retained distribution (higher is better), and **u-Acc** as the accuracy on the unlearning target set \mathcal{D}_u (lower is better). To quantify knowledge resurfacing under continued training, we report RR defined in Eq. (8) (lower is better).

For HSViT (Pat-50), we adopt communication rounds as the primary efficiency metric, reflecting the dominant bottleneck in FL and FU [17]. The total unlearning overhead is defined as $T_{\text{tot}} = T_{\text{U}} + T_{\text{P}}$, where: (i) *unlearning rounds* T_{U} represents the period where unlearning clients must participate to facilitate forgetting; (ii) *recovering rounds* T_{P} denotes the subsequent rounds on remaining clients to restore model utility. The retraining baseline reports the total rounds to train from scratch on the remaining data.

5.2 Main Results

Non-IID client unlearning under two-stage deployment. Table 1 shows that Phase U alone can be misleading: several baselines reduce u-Acc to near-zero by the end of Phase U, yet the removed influence can resurface once standard FL training resumes on the remaining clients in Phase C. This knowledge resurfacing is pronounced for representative baselines (e.g., FedAU and FedOSD), whereas LETHE keeps u-Acc consistently low throughout Phase C across architectures and client scales, demonstrating persistent forgetting under continued training.

Sample-level and class-level unlearning. Table 2 further confirms LETHE’s effectiveness across unlearning granularities. For sample unlearning (1% ~ 20%), LETHE consistently drives u-Acc to a low level by the end of Phase U and keeps it low after Phase C, indicating minimal knowledge resurfacing under continued training. In contrast, FedAU exhibits pronounced rebound in Phase C, and NoT also shows non-negligible increases of u-Acc, suggesting residual influence of knowledge unlearned. For class unlearning, LETHE matches the retraining baseline, achieving and maintaining near-zero u-Acc across both phases.

Observations on “Rollback”. Motivated by task-vector diagnostics [18], we analyze whether continued training rolls back the unlearning displacement in Phase C. The unlearning-induced displacement $w_{pre} - w_{un}$ is defined as the “rollback vector” and, at round t of Phase C, we denote the global update by Δw_t . We

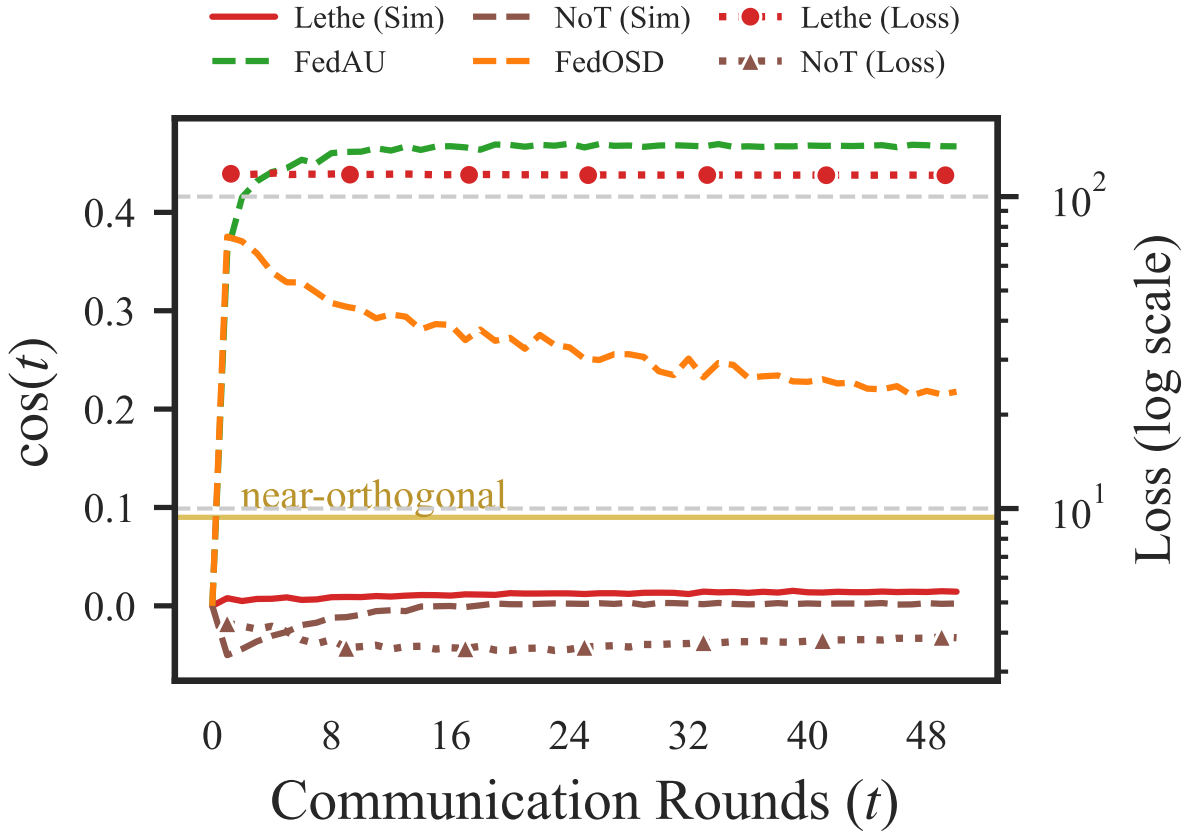


Figure 4: Trace of the update’s correlation with the rollback vector and u-set loss during continued training (Phase C). Per-round cosine similarity $\cos(t)$ measures how the Phase C update Δw_t aligns with the rollback vector (undoing unlearning).

compute

$$\cos(t) \triangleq \frac{\langle \Delta w_t, w_{\text{pre}} - w_{\text{un}} \rangle}{\|\Delta w_t\|_2 \|w_{\text{pre}} - w_{\text{un}}\|_2}. \quad (14)$$

$\cos(t) > 0$ indicates that Phase C updates align with the rollback vector $w_{\text{pre}} - w_{\text{un}}$, i.e., drifting back toward w_{pre} and partially undoing unlearning. In contrast, $\cos(t) \approx 0$ suggests near-orthogonality and thus avoids rollback. Following prior cosine-based diagnostics that treat small values (e.g., ≈ 0.09) as near-orthogonal [18], we adopt $\cos(t) < 0.1$ as a conservative threshold for *weak rollback*. In our results shown in Fig. 4, LETHE stays essentially at zero throughout, indicating negligible rollback under continued training. FedAU and FedOSD have their Phase-C update positively correlated with the rollback vector, while LETHE stays near-orthogonal (< 0.09), indicating suppressed rollback. NoT’s update is slightly negative, yet its unlearning-set loss stays low (right axis), revealing substantial residual influence on \mathcal{D}_u .

Client-level Unlearning and Resurfacing Rate. Table 3 summarizes resurfacing severity using RR across scenarios. Overall, LETHE attains the lowest or near-lowest RR on both Non-IID client unlearning and sample/class unlearning settings, indicating consistently strong stability under continued training. This trend also holds on HSViT, further supporting a favorable stability–utility trade-off.

Table 3: Resurfacing Rates (RR, %) and unsuccessful forgetting (UF, %). **Lower is better** for both metrics. For cases where unlearning is unsuccessful, we report UF (followed by u-Acc during the phase U). Note that FedOSD is designed exclusively for client-level unlearning; thus, results for sample-level and class-level scenarios are not applicable (-). The best results are marked in **bold**.

Setting / Task	FedAU	FedOSD	NoT	ours
Client Unlearning				
LeNet5 (Pat-10)	36.03	10.48	0.00	0.00
LeNet5 (Pat-50)	49.56	3.59	0.00	0.12
ResNet18 (Pat-10)	94.17	62.63	UF(21.89)	0.15
ResNet18 (Pat-50)	99.85	74.18	UF(35.78)	1.15
HSVIT (Pat-50)	23.42	69.29	0.05	0.38
Sample Unlearning				
1% Samples	64.44	–	UF(21.98)	0.19
5% Samples	87.38	–	UF(30.27)	0.33
10% Samples	90.29	–	UF(15.31)	0.83
20% Samples	92.26	–	UF(23.42)	0.35
Class Unlearning				
Client-10	0.00	–	10.19	0.00
Client-50	0.00	–	3.11	0.00

5.3 Ablation Studies

To validate the contribution of each component in the LETHE *Reshape–Rectify–Restore* pipeline, we evaluate four variants under the same data split as the main method. We report only: (i) the number of communication rounds in Phase U (unlearning overhead), and (ii) the Resurfacing Rate (RR) measured during Phase C.

(I) w/o Adapter (Backbone-based Probe). We remove the adapter entirely and compute the probe direction Δ_t^u via standard local training on \mathcal{D}_u with the same probe hyperparameters (local steps/optimizer) as in the main method, directly updating the backbone. This tests whether a dedicated lightweight module is necessary to produce a faithful probe direction.

(II) w/o Rectify (No-Correction Baseline). We keep *Reshape* and compute Δ_t^u as usual, but disable *Rectify* by setting $\tilde{\Delta}_t \leftarrow \Delta_t^r$. This baseline isolates the effect of conflict-aware rectification in suppressing knowledge resurfacing during Phase C.

(III) w/o Conditionality (Unconditional Rectify). We remove the layer-wise alignment check and apply $\tilde{\Delta}_t^{(\ell)} = \Delta_t^{r,(\ell)} - \gamma \Delta_t^{u,(\ell)}$ for all layers regardless of the sign of $\text{sim}^{(\ell)}$. This tests the necessity of conflict-aware gating versus blind subtraction.

(IV) Adapter Removability (Diagnostic) We do not remove the (frozen) adapter in *Restore*. Instead, we keep it attached when entering Phase C and throughout continued training, and evaluate the continued model with the adapter. Since this changes model capacity, we treat this variant as diagnostic for whether the unlearning effect relies on the adapter during Phase C.

Ablation results. Table 4 confirms the contribution of each module in the LETHE Reshape–Rectify–Restore pipeline in terms of unlearning efficiency (Phase U rounds) and persistence under continued training (Phase C stability). Disabling Rectify (II) consistently leads to unsuccessful forgetting (UF), indicating that conflict-aware correction is necessary for reliable unlearning. Removing the probe adapter (I) is sometimes feasible but typically increases Phase U rounds when the forget signal is weak, showing that the probe stabilizes the estimated unlearning direction. Dropping conditionality (III) degrades overall performance, suggesting that alignment-aware gating is preferable to unconditional subtraction. Finally, keeping the adapter during

Table 4: Resurfacing Rates (RR, %) and unsuccessful forgetting (UF).

Setting	Metric	(I)	(II)	(III)	(IV)	LETHE
LeNet5	rounds	9	23	9	24	8
	RR (%)	0.63	82.5	0.53	0.47	0.00
ResNet18	rounds	22	10	28	47	22
	RR (%)	0.72	94.7	0.72	0.65	0.69
HSViT	rounds	30	16	45	39	30
	RR (%)	0.83	UF	0.90	0.91	0.82
Sample	rounds	17	2	5	6	5
	RR (%)	0.00	UF	0.00	0.00	0.00
Class	rounds	13	18	19	18	18
	RR (%)	0.00	UF	0.00	0.00	0.00

Phase C (IV) brings no benefit and may incur extra overhead, supporting its removal after unlearning.

6 Conclusion

We study federated unlearning in a deployment-realistic setting where deletion requests are interleaved with continued federated training on remaining clients. We identify knowledge resurfacing as a key failure mode: the removed influence can resurface within a few additional communication rounds. To address this, we first introduce *Resurfacing Rate* (RR) to quantify the diminishing effect of forgetting during continued training and provide in-depth theoretical analysis. Then we propose LETHE, an FU method that follows a Reshape–Rectify–Restore pipeline and supports persistent unlearning at sample, class and client levels. With extensive experiments over a rich set of models and datasets, we demonstrate that many SOTA methods are prone to knowledge resurfacing, whilst LETHE unlearns efficiently and keeps RR at a very low level throughout the follow-up training. We believe our method offers an efficient and effective solution to persistent FU. In the future we plan to further introduce automated calibration of rectification strength with stronger theoretical guarantee.

Impact Statement

This paper presents work whose goal is to advance the field of Machine Learning. There are many potential societal consequences of our work, none of which we feel must be specifically highlighted here.

References

- [1] Deng, J., Dong, W., Socher, R., Li, L.-J., Li, K., and Fei-Fei, L. ImageNet: A large-scale hierarchical image database. In *Proceedings of the IEEE Conference on Computer Vision and Pattern Recognition (CVPR)*, pp. 248–255, 2009. doi: 10.1109/CVPR.2009.5206848.
- [2] Gao, X., Ma, X., Wang, J., Sun, Y., Li, B., Ji, S., Cheng, P., and Chen, J. Verifi: Towards verifiable federated unlearning. *IEEE Transactions on Dependable and Secure Computing*, 21(6):5720–5736, 2024.

- [3] Gu, H., Zhu, G., Zhang, J., Zhao, X., Han, Y., Fan, L., and Yang, Q. Unlearning during learning: An efficient federated machine unlearning method. *arXiv preprint arXiv:2405.15474*, 2024.
- [4] Halimi, A., Kadhe, S., Rawat, A., and Baracaldo, N. Federated unlearning: How to efficiently erase a client in fl?, 2022. *URL https://arxiv.org/abs/2207.05521*, 2022.
- [5] He, K., Zhang, X., Ren, S., and Sun, J. Deep residual learning for image recognition. In *Proceedings of the IEEE conference on computer vision and pattern recognition*, pp. 770–778, 2016.
- [6] Hsu, T.-M. H., Qi, H., and Brown, M. Measuring the effects of non-identical data distribution for federated visual classification. *arXiv preprint arXiv:1909.06335*, 2019.
- [7] Hu, S., Fu, Y., Wu, Z. S., and Smith, V. Unlearning or obfuscating? jogging the memory of unlearned llms via benign relearning. In *International Conference on Learning Representations (ICLR)*, 2025. *URL https://openreview.net/forum?id=fMNRYBvcQN*.
- [8] Khalil, Y. H., Brunswic, L., Lamghari, S., Li, X., Beitollahi, M., and Chen, X. Not: Federated unlearning via weight negation. In *Proceedings of the Computer Vision and Pattern Recognition Conference*, pp. 25759–25769, 2025.
- [9] Krizhevsky, A. Learning multiple layers of features from tiny images. Technical Report TR-2009, University of Toronto, 2009.
- [10] Le, Y. and Yang, X. Tiny imagenet visual recognition challenge. *CS 231N*, 7(7):3, 2015.
- [11] LeCun, Y., Bottou, L., Bengio, Y., and Haffner, P. Gradient-based learning applied to document recognition. *Proceedings of the IEEE*, 86(11):2278–2324, 2002.
- [12] Liu, G., Ma, X., Yang, Y., Wang, C., and Liu, J. Federated unlearning. *arXiv preprint arXiv:2012.13891*, 2020.
- [13] Liu, G., Ma, X., Yang, Y., Wang, C., and Liu, J. Federaser: Enabling efficient client-level data removal from federated learning models. In *2021 IEEE/ACM 29th International Symposium on Quality of Service (IWQOS)*, pp. 1–10. IEEE, 2021.
- [14] McMahan, B., Moore, E., Ramage, D., Hampson, S., and y Arcas, B. A. Communication-efficient learning of deep networks from decentralized data. In *Artificial intelligence and statistics*, pp. 1273–1282, 2017.
- [15] Meerza, S. I. A., Sadovnik, A., and Liu, J. Confuse: Confusion-based federated unlearning with salience exploration. In *2024 IEEE Computer Society Annual Symposium on VLSI (ISVLSI)*, pp. 427–432. IEEE, 2024.
- [16] Pan, Z., Wang, Z., Li, C., Zheng, K., Wang, B., Tang, X., and Zhao, J. Federated unlearning with gradient descent and conflict mitigation. In *Proceedings of the AAAI Conference on Artificial Intelligence*, volume 39, pp. 19804–19812, 2025.
- [17] Tan, Q., Che, X., Wu, S., Qian, Y., and Tao, Y. Privacy amplification for wireless federated learning with renyi differential privacy and subsampling. *Electr Res Arch*, 31(11):7021–7039, 2023.
- [18] Wang, C., Zhang, Y., Jia, J., Ram, P., Wei, D., Yao, Y., Pal, S., Baracaldo, N., and Liu, S. Invariance makes llm unlearning resilient even to unanticipated downstream fine-tuning. *arXiv preprint arXiv:2506.01339*, 2025.

- [19] Xu, C., Li, C.-T., Lim, C. P., and Creighton, D. Hsvit: Horizontally scalable vision transformer, 2024.
- [20] Yu, B., Mao, W., Lv, Y., Zhang, C., and Xie, Y. A survey on federated learning in data mining. *Wiley Interdisciplinary Reviews: Data Mining and Knowledge Discovery*, 12(1):e1443, 2022.
- [21] Yu, T., Kumar, S., Gupta, A., Levine, S., Hausman, K., and Finn, C. Gradient surgery for multi-task learning. In *Advances in Neural Information Processing Systems (NeurIPS)*, 2020. doi: 10.48550/arXiv.2001.06782. URL <https://arxiv.org/abs/2001.06782>. Also known as PCGrad.
- [22] Zhang, L., Zhu, T., Zhang, H., Xiong, P., and Zhou, W. Fedrecovery: Differentially private machine unlearning for federated learning frameworks. *IEEE Transactions on Information Forensics and Security*, 18:4732–4746, 2023.
- [23] Zhong, Z., Bao, W., Wang, J., Zhang, S., Zhou, J., Lyu, L., and Lim, W. Y. B. Unlearning through knowledge overwriting: Reversible federated unlearning via selective sparse adapter. In *Proceedings of the Computer Vision and Pattern Recognition Conference*, pp. 30661–30670, 2025.

A Proof of Proposition 4.1

Proof. Let $w_0 = w_{\text{pre}}$ and define the reference unlearning gradient $g_u := \nabla \mathcal{L}_u(w_{\text{pre}})$. Since \mathcal{L}_u is β -smooth, for any x, y ,

$$\mathcal{L}_u(y) \leq \mathcal{L}_u(x) + \langle \nabla \mathcal{L}_u(x), y - x \rangle + \frac{\beta}{2} \|y - x\|^2. \quad (15)$$

Apply (15) with $x = w_t$ and $y = w_{t+1} = w_t - \eta g_r^{(t)}$:

$$\mathcal{L}_u(w_{t+1}) \leq \mathcal{L}_u(w_t) - \eta \langle \nabla \mathcal{L}_u(w_t), g_r^{(t)} \rangle + \frac{\beta \eta^2}{2} \|g_r^{(t)}\|^2. \quad (16)$$

Taking expectation and using $\|g_r^{(t)}\| \leq G$ gives

$$\mathbb{E}[\mathcal{L}_u(w_{t+1})] \leq \mathbb{E}[\mathcal{L}_u(w_t)] - \eta \mathbb{E}[\langle \nabla \mathcal{L}_u(w_t), g_r^{(t)} \rangle] + \frac{\beta \eta^2 G^2}{2}. \quad (17)$$

We split the unlearning gradient into the reference term at w_{pre} and a drift term:

$$\nabla \mathcal{L}_u(w_t) = g_u + (\nabla \mathcal{L}_u(w_t) - g_u).$$

Hence

$$\mathbb{E}[\langle \nabla \mathcal{L}_u(w_t), g_r^{(t)} \rangle] = \mathbb{E}[\langle g_u, g_r^{(t)} \rangle] + \mathbb{E}[\langle \nabla \mathcal{L}_u(w_t) - g_u, g_r^{(t)} \rangle]. \quad (18)$$

To bound the drift term, β -smoothness implies $\nabla \mathcal{L}_u$ is β -Lipschitz:

$$\|\nabla \mathcal{L}_u(w_t) - g_u\| = \|\nabla \mathcal{L}_u(w_t) - \nabla \mathcal{L}_u(w_{\text{pre}})\| \leq \beta \|w_t - w_{\text{pre}}\|.$$

Moreover, using $w_{k+1} = w_k - \eta g_r^{(k)}$ and $w_0 = w_{\text{pre}}$,

$$w_t - w_{\text{pre}} = -\eta \sum_{k=0}^{t-1} g_r^{(k)} \Rightarrow \|w_t - w_{\text{pre}}\| \leq \eta \sum_{k=0}^{t-1} \|g_r^{(k)}\| \leq \eta t G.$$

Therefore,

$$\|\nabla \mathcal{L}_u(w_t) - g_u\| \leq \beta \eta t G. \quad (19)$$

By Cauchy–Schwarz and $\|g_r^{(t)}\| \leq G$,

$$\left| \langle \nabla \mathcal{L}_u(w_t) - g_u, g_r^{(t)} \rangle \right| \leq \|\nabla \mathcal{L}_u(w_t) - g_u\| \|g_r^{(t)}\| \leq \beta \eta t G^2. \quad (20)$$

Combining (17), (18), and (20) yields

$$\mathbb{E}[\mathcal{L}_u(w_{t+1})] \leq \mathbb{E}[\mathcal{L}_u(w_t)] - \eta \mathbb{E}[\langle g_u, g_r^{(t)} \rangle] + \beta \eta^2 t G^2 + \frac{\beta \eta^2 G^2}{2}. \quad (21)$$

Summing (21) over $t = 0, 1, \dots, T-1$ gives

$$\mathbb{E}[\mathcal{L}_u(w_T)] \leq \mathcal{L}_u(w_{\text{pre}}) - \eta \sum_{t=0}^{T-1} \mathbb{E}[\langle g_u, g_r^{(t)} \rangle] + \beta \eta^2 G^2 \sum_{t=0}^{T-1} t + \frac{\beta \eta^2 G^2}{2} T.$$

Using Assumption (iii) in Proposition 4.1, $\frac{1}{T} \sum_{t=0}^{T-1} \mathbb{E}[\langle g_u, g_r^{(t)} \rangle] \geq \rho$ (i.e., $\sum_{t=0}^{T-1} \mathbb{E}[\langle g_u, g_r^{(t)} \rangle] \geq \rho T$), and $\sum_{t=0}^{T-1} t = \frac{T(T-1)}{2}$, we obtain

$$\begin{aligned} \mathbb{E}[\mathcal{L}_u(w_T)] &\leq \mathcal{L}_u(w_{\text{pre}}) - \eta \rho T + \beta \eta^2 G^2 \cdot \frac{T(T-1)}{2} + \frac{\beta \eta^2 G^2}{2} T \\ &= \mathcal{L}_u(w_{\text{pre}}) - \eta \rho T + \frac{\beta \eta^2 G^2}{2} T^2, \end{aligned}$$

which proves the stated bound.

Finally, $\mathbb{E}[\mathcal{L}_u(w_T)] < \mathcal{L}_u(w_{\text{pre}})$ holds whenever $-\eta \rho T + \frac{\beta \eta^2 G^2}{2} T^2 < 0$, equivalently $T < \frac{2\rho}{\beta \eta G^2}$. \square

B Additional Proofs

B.1 Proof of Proposition 4.2

Setup and linearization. Let $\mathcal{L}_u(\mathbf{w})$ and $\mathcal{L}_r(\mathbf{w})$ be the empirical risks on the forget and retain data, respectively. We consider a single round t with the server update $\mathbf{w}_{t+1} = \mathbf{w}_t + \tilde{\Delta}_t$, where $\tilde{\Delta}_t$ is formed layer-wise. We use the standard first-order local-update approximation (small local step size):

$$\Delta_t^{u,(\ell)} = -\eta_u \nabla_{\mathbf{w}^{(\ell)}} \mathcal{L}_u(\mathbf{w}_t) + \mathcal{O}(\eta_u^2), \quad \Delta_t^{r,(\ell)} = -\eta_r \nabla_{\mathbf{w}^{(\ell)}} \mathcal{L}_r(\mathbf{w}_t) + \mathcal{O}(\eta_r^2). \quad (22)$$

A first-order condition for increasing \mathcal{L}_u . A first-order Taylor expansion of \mathcal{L}_u yields

$$\mathcal{L}_u(\mathbf{w}_{t+1}) - \mathcal{L}_u(\mathbf{w}_t) = \sum_{\ell} \left\langle \nabla_{\mathbf{w}^{(\ell)}} \mathcal{L}_u(\mathbf{w}_t), \tilde{\Delta}_t^{(\ell)} \right\rangle + \mathcal{O}\left(\sum_{\ell} \|\tilde{\Delta}_t^{(\ell)}\|^2\right). \quad (23)$$

Using (22), we have $\nabla_{\mathbf{w}^{(\ell)}} \mathcal{L}_u(\mathbf{w}_t) = -\Delta_t^{u,(\ell)} / \eta_u + \mathcal{O}(\eta_u)$, hence

$$\mathcal{L}_u(\mathbf{w}_{t+1}) - \mathcal{L}_u(\mathbf{w}_t) = -\frac{1}{\eta_u} \sum_{\ell} \left\langle \Delta_t^{u,(\ell)}, \tilde{\Delta}_t^{(\ell)} \right\rangle + \mathcal{O}\left(\sum_{\ell} \|\tilde{\Delta}_t^{(\ell)}\|^2\right). \quad (24)$$

Therefore, a sufficient first-order condition for *increasing* the forget risk is $\langle \Delta_t^{u,(\ell)}, \tilde{\Delta}_t^{(\ell)} \rangle \leq 0$ for all layers ℓ .

Proof of (i) (Forgetting correctness). We verify $\langle \Delta_t^{u,(\ell)}, \tilde{\Delta}_t^{(\ell)} \rangle \leq 0$ under both branches of the rule.

Non-positive alignment branch. If $\langle \Delta_t^{r,(\ell)}, \Delta_t^{u,(\ell)} \rangle \leq 0$, LETHE uses $\tilde{\Delta}_t^{(\ell)} = -\Delta_t^{u,(\ell)}$, hence

$$\left\langle \Delta_t^{u,(\ell)}, \tilde{\Delta}_t^{(\ell)} \right\rangle = -\|\Delta_t^{u,(\ell)}\|^2 \leq 0. \quad (25)$$

Positive alignment branch. If $\langle \Delta_t^{r,(\ell)}, \Delta_t^{u,(\ell)} \rangle > 0$, LETHE uses $\tilde{\Delta}_t^{(\ell)} = \Delta_t^{r,(\ell)} - \gamma \Delta_t^{u,(\ell)}$, so

$$\left\langle \Delta_t^{u,(\ell)}, \tilde{\Delta}_t^{(\ell)} \right\rangle = \left\langle \Delta_t^{u,(\ell)}, \Delta_t^{r,(\ell)} \right\rangle - \gamma \|\Delta_t^{u,(\ell)}\|^2. \quad (26)$$

If $\|\Delta_t^{u,(\ell)}\| > 0$ and

$$\gamma \geq \frac{\langle \Delta_t^{u,(\ell)}, \Delta_t^{r,(\ell)} \rangle}{\|\Delta_t^{u,(\ell)}\|^2}, \quad (27)$$

then (26) implies $\langle \Delta_t^{u,(\ell)}, \tilde{\Delta}_t^{(\ell)} \rangle \leq 0$.

Combining the two branches, we have $\langle \Delta_t^{u,(\ell)}, \tilde{\Delta}_t^{(\ell)} \rangle \leq 0$ for all ℓ , and thus (24) gives $\mathcal{L}_u(\mathbf{w}_{t+1}) \geq \mathcal{L}_u(\mathbf{w}_t)$ to first order. This proves (i).

Proof of (ii) (Utility non-adversarial in the non-positive alignment case). If $\langle \Delta_t^{r,(\ell)}, \Delta_t^{u,(\ell)} \rangle \leq 0$, then $\tilde{\Delta}_t^{(\ell)} = -\Delta_t^{u,(\ell)}$, and therefore

$$\left\langle \Delta_t^{r,(\ell)}, \tilde{\Delta}_t^{(\ell)} \right\rangle = -\left\langle \Delta_t^{r,(\ell)}, \Delta_t^{u,(\ell)} \right\rangle \geq 0, \quad (28)$$

which is exactly the claimed non-adversariality. \square

C Experimental Setting

Models, datasets, and federation scale. We evaluate on MNIST [11] with LeNet-5 [11], CIFAR-10 [9] with ResNet-18 [5], and Tiny-ImageNet [1, 10] with HSViT [19]. We consider two federation scales: **Pat-10** and **Pat-50**, which denote training with $K = 10$ clients and $K = 50$ clients, respectively.

Data partition (IID). For the IID setting, the global training set is partitioned across K clients with *equal* sample sizes. We use a stratified uniform split to match the class histogram across clients as closely as possible, eliminating the impact of quantity skew. The quantitative results under the IID partition are summarized in Table 5, and the corresponding resurfacing rates (RR) are computed from Table 5 and reported in Table 6.

Unlearning task (client unlearning). Unless otherwise specified, we study **client unlearning**: we designate one client as the unlearning client and denote its local dataset as \mathcal{D}_u ; all remaining clients form the remaining dataset \mathcal{D}_r . We evaluate the utility of the unlearned model by **t-Acc** (test accuracy on the clean held-out test set), and evaluate forgetting by **u-Acc** (accuracy on the forget evaluation set constructed from \mathcal{D}_u).

Hyper-parameters. For all experiments, we fix the learning rate $\eta = 0.001$ and the momentum factor to 0.9. Unless otherwise specified, each selected client performs one local epoch per communication round ($E = 1$). We use batch size $B = 64$ for LeNet-5 and ResNet-18, and $B = 512$ for HSViT for stability and hardware efficiency. All results are averaged over three random seeds $\{2023, 2024, 2025\}$. For continued training in Phase C, we run standard FedAvg on the *remaining* clients only.

Phase reporting. Superscripts U and C report results measured after Phase U (immediately after unlearning) and after Phase C, respectively. For HSViT (Pat-50), communication rounds are reported as T_U/T_P , where T_U is the number of unlearning-stage rounds and T_P is the number of additional post-unlearning rounds used for utility recovery (before/within continued training, depending on the method).

D Correlation Penalty γ

We analyze how varying γ affects the total number of rounds T_{tot} . The experimental results in Fig. 5 show that: when the forgetting target is larger (e.g., class-level or client-level), a moderate correlation penalty ($\gamma = 0.3$) yields the lowest total rounds; when the forgetting target is smaller (sample-level), a stronger penalty is beneficial and the optimal setting shifts to $\gamma = 1.5$. Intuitively, larger unlearning sets already provide a strong forgetting signal and over-penalization can slow recovery, whereas smaller forget sets need stronger rectification to suppress resurfacing without excessive extra rounds.

Table 5: Performance comparison of different algorithms under the **IID setting**. **u-Acc** lower is better and **t-Acc** higher is better. w_{pre} denotes the model before unlearning; superscripts U and C report results measured after Phase U and after Phase C, respectively. For HSViT (Pat-50), communication rounds are reported as T_U/T_P . The best results are marked in **bold**.

Algorithm	LeNet-5				ResNet-18				HSViT		
	Pat-10		Pat-50		Pat-10		Pat-50		Pat-50		
	u-Acc ↓	t-Acc	T_U/T_P	u-Acc ↓	t-Acc						
w_{pre}	96.45±1.61	98.79	97.64±1.61	98.05	96.29±0.71	74.58	94.89±0.66	73.63	-	94.48±3.10	48.82
Retraining	0.14±0.05	98.55	0.34±0.04	97.10	2.16±0.24	76.42	2.23±0.49	71.48	1000	0.30±0.14	52.15
FedEraser	0.09±0.05	99.05	0.16±0.12	98.65	1.32±0.23	78.45	1.56±0.25	78.47	-	-	-
FedAU ^U	0.07±0.05	96.86	0.37±0.27	96.81	0.30±0.23	77.97	0.56±0.15	73.72	57/0	0.17±0.09	43.90
FedOSD ^U	0.79±0.15	98.86	0.65±0.20	97.93	3.66±2.49	81.00	0.41±0.14	77.18	10/20	97.40±0.48	48.92
NoT ^U	0.08±0.02	97.60	0.44±0.36	94.93	42.37±7.32	78.18	8.66±2.55	72.71	0/31	0.23±0.26	44.82
ours ^U	0.48±0.02	96.79	0.56±0.14	96.40	0.25±0.17	80.80	0.15±0.05	76.26	10/11	0.22±0.02	49.24
After continued training (Phase C)											
FedAU ^C	15.71±0.91	99.03	41.68±9.73	98.32	79.00±2.13	82.01	79.93±5.93	77.99	-	44.84±2.28	50.30
FedOSD ^C	7.15±0.45	99.01	10.56±3.70	98.44	21.10±6.55	81.84	19.66±4.45	77.93	-	50.43±20.94	50.72
NoT ^C	0.38±0.40	98.94	0.47±0.33	97.74	54.42±5.76	78.83	13.21±3.52	74.75	-	0.18±0.02	51.01
ours ^C	0.25±0.08	98.90	0.41±0.18	98.15	0.39±0.27	81.16	0.48±0.40	77.31	-	0.38±0.26	51.60

Table 6: Resurfacing Rates (RR, %) and unsuccessful forgetting (UF, %). **Lower is better** for both metrics. For cases where unlearning is unsuccessful, we report UF (defined as the u-Acc during the phase U) to quantify residual information. The best results are marked in **bold**.

Setting / Task	FedAU	FedOSD	NoT	Ours
Client Unlearning				
LeNet5 (Pat-10)	16.23	6.65	0.31	0.00
LeNet5 (Pat-50)	42.47	10.22	0.03	0.00
ResNet18 (Pat-10)	81.99	18.83	UF(42.37)	0.15
ResNet18 (Pat-50)	84.14	20.37	UF(8.66)	0.35
HSViT (Pat-50)	47.36	UF(97.40)	0.00	0.17

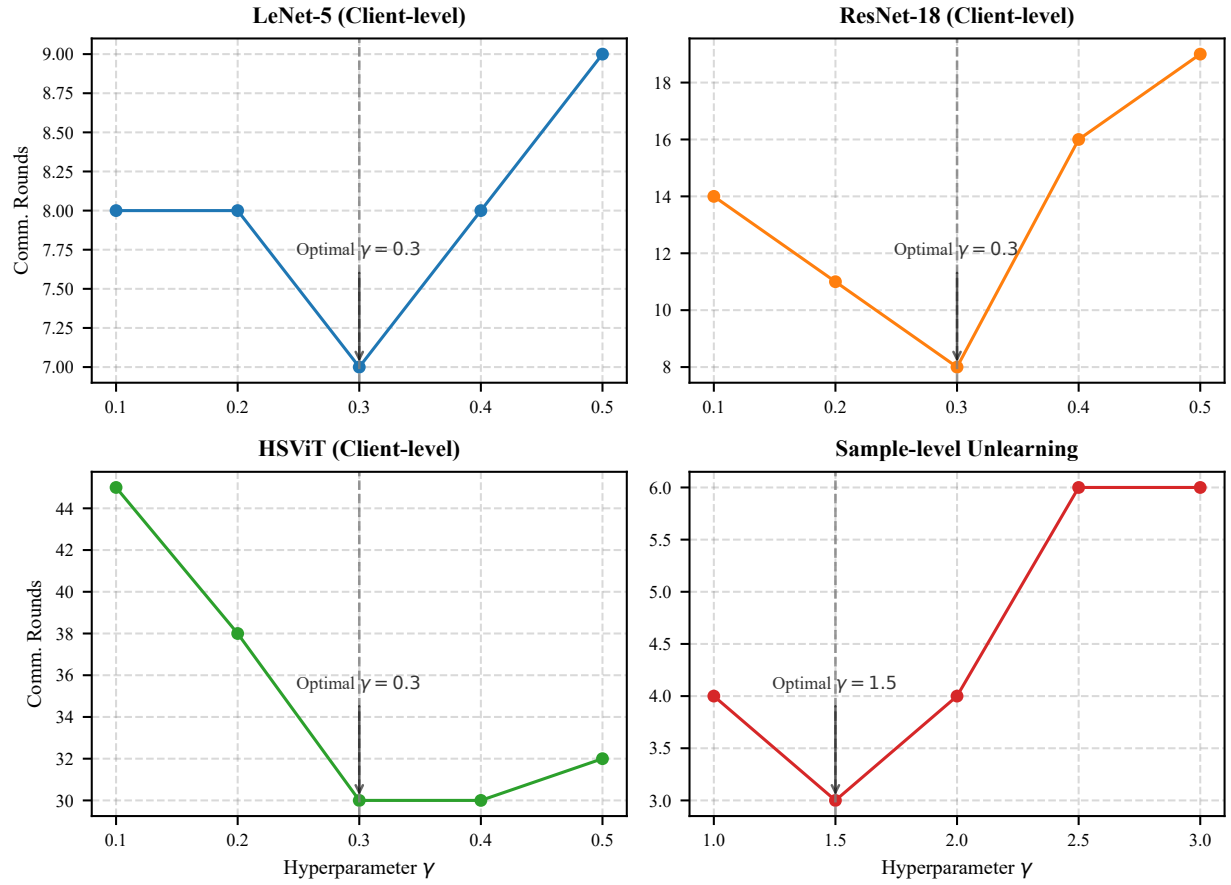


Figure 5: Hyperparameter study of γ . Communication rounds (lower is better) versus the correlation penalty γ . Dashed lines mark the chosen values: $\gamma = 0.3$ for client-level and $\gamma = 1.5$ for sample-level unlearning.